ChemPubSoc Europe

DOI: 10.1002/cmdc.201500534

CHEMMEDCHEM Full Papers

Different Binding Modes of Small and Large Binders of GAT1

Thomas Wein,[a] Marilena Petrera,[b] Lars Allmendinger,[a] Georg Höfner,[a] Jörg Pabel,[a] and Klaus T. Wanner*[a]

Well-known inhibitors of the γ-aminobutyric acid (GABA) transporter GAT1 share a common scaffold of a small cyclic amino acid linked by an alkyl chain to a moiety with two aromatic rings. Tiagabine, the only FDA-approved GAT1 inhibitor, is a typical example. Some small amino acids such as (*R*)-nipecotic acid are medium-to-strong binders of GAT1, but similar compounds, such as proline, are very weak binders. When substituted with 4,4-diphenylbut-3-en-1-yl (DPB) or 4,4-bis(3-methylthiophen-2-yl)but-3-en-1-yl (BTB) groups, the resulting compounds have similar pK_i and pIC_{50} values, even though the pure amino acids have very different values. To investigate if small amino acids and their substituted counterparts share a similar binding mode, we synthesized butyl-, DPB-, and BTB-substituted derivatives of small amino acids. Supported by the results of docking studies, we propose different binding modes not only for unsubstituted und substituted, but also for strong- and weak-binding amino acids. These data lead to the conclusion that following a fragment-based approach, not pure but *N*-butyl-substituted amino acids should be used as starting points, giving a better estimate of the activity when a BTB or DPB substituent is added.

Introduction

γ-Aminobutyric acid (GABA) is the most important inhibitory neurotransmitter in the mammalian brain. It plays a major role in the regulation of neuronal activity throughout the central nervous system (CNS). The inhibitory action of GABA in the synaptic cleft is terminated by the reuptake of GABA in neurons and astroglial cells via GABA transport proteins. Four subtypes of GABA transporters[1] (GATs) are currently known: only GAT1 and GAT3 are present in the CNS in significant amounts, whereas GAT2 and BGT1 are located primarily in the liver and kidneys.[2] When cloned from mice these GABA transporters are generally termed mGAT1, mGAT2, mGAT3, and mGAT4.[3] Herein we use the nomenclature suggested by the Human Genome Organization (HUGO) in which the corresponding human GABA transport proteins are denoted as GAT1 (encoding gene: *SLC6A1*), BGT1 (*SLC6A12*), GAT2 (*SLC6A13*), and GAT3 (*SLC6A11*), respectively.[4] The GATs are members of the *SLC6* gene family of sodium- and chloride-dependent neurotransmitter transporters, including transporters for glycine, dopamine, norepinephrine, and serotonin,[5] which are of considerable medical interest. These transporters ensure that the concentrations of the neurotransmitters in the synapse are low, so that post-synaptic receptors can detect neurotransmitter molecules upon exocytotic release from pre-synaptic neurons. Inhibition of neurotransmitter uptake from the synaptic cleft increases the level of neurotransmitter in the synaptic cleft and enhances synaptic transmission. Hence, neurotransmitter transporters provide important targets for therapeutic intervention. Inhibition of GABA uptake has been recognized as a therapeutic strategy for the treatment of epileptic disorders,[6] for example. Since the 1970s and supported in the 1990s by the first cloning of human[7] and rat[8] brain GABA transporters, a huge medicinal chemistry effort aimed at the development of GAT inhibitors has begun, resulting in tiagabine {(*R*)-**1**: (3*R*)-1-[4,4-bis(3-methylthiophen-2-yl)but-3-en-1-yl]piperidine-3-carboxylic acid}, as the only US Food and Drug Administration (FDA)-approved GAT inhibitor (selective for GAT1) for the therapy of epilepsy.[9] Several other GAT1 inhibitors such as NO711[10] (**2**), SKF89976A[11] [(*R*)-**3**], and CI966[12] (**4**), sharing common scaffolds of a small cyclic amino acid linked by an alkyl or heteroalkyl chain to a lipophilic substructure with two aromatic rings (Figure 1), have been identified without reaching approved drug status. In addition, tiagabine [(*R*)-**1**] is being investigated for other possible indications such as the treatment of general anxiety[13] and depression.[14]

As early as the 1970s (*R*,*S*)-nipecotic acid [(*R*,*S*)-**5a**] and guvacine (**6a**) were found to be inhibitors of GABA uptake in neuronal and astroglial cell cultures,[6,15] where (*R*)-nipecotic acid [(*R*)-**5a**] was known to be a more potent inhibitor than the *S* isomer [(*S*)-**5a**] for GABA uptake in rat brain slices.[15c] The inhibitory effect on GABA transport of 2-[(3*S*)-pyrrolidin-3-yl]acetic acid[16] [(*S*)-**7a**] (homo-β-proline) has also been known for a long time. Other cyclic amino acids very similar to nipecotic

[a] Dr. T. Wein, Dr. L. Allmendinger, Dr. G. Höfner, Dr. J. Pabel, Prof. Dr. K. T. Wanner
Department for Pharmacy—Center for Drug Research
Ludwig-Maximilians-Universität München
Butenandtstr. 7-13, 81377 Munich (Germany)
E-mail: klaus.wanner@cup.uni-muenchen.de

[b] Dr. M. Petrera
Galliera Hospital, Mura delle Cappuccine 14, 16128 Genova (Italy)

Supporting information for this article is available on the WWW under http://dx.doi.org/10.1002/cmdc.201500534.

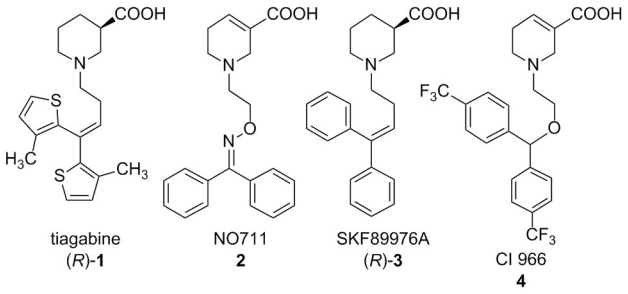

Figure 1. Structures of known GABA uptake inhibitors.

acid or guvacine, such as (*R*)- and (*S*)-proline [(*R*)-**8a** and (*S*)-**8a**] or (*R*)- and (*S*)-2-(pyrrolidin-2-yl)acetic acid[17] [(*R*)-**9a** and (*S*)-**9a**] (homoproline) show only weak or no inhibitory potential on GABA uptake. However, adding bulky lipophilic groups to the nitrogen atom increases the inhibitory potential of these small amino acids by several orders of magnitude,[16c,17,18] nearly reaching the potency of tiagabine (Table 1, entry 33). This is true for the uptake inhibition values (pIC_{50}) as well as for the binding activities (pK_i) listed in Table 1.

In 2005 the first X-ray structure of a bacterial leucine transporter (LeuT) homologue to the SLC6 transporters was reported,[19] giving insight into the three-dimensional (3D) structure of this important class of transport proteins and serving as a foundation for structure-based design through homology modeling of the other SLC6 proteins. The X-ray structure of LeuT revealed 12 transmembrane helices (TMs) of which the protein core consists of segments TM1–TM5 and TM6–TM10, which are related by a pseudo-twofold axis located in the membrane plane. The substrate leucine could be clearly identified in an inner binding site called the S1 site almost in the middle of the transmembrane protein, which includes two bound sodium ions, of which one forms direct interactions with the substrate. The S1 site is closed to the extracellular side by a pair of aromatic residues—Tyr108 and Phe253—and a salt bridge formed by Arg30 and Asp404. Another cavity is located above these gating residues, called the S2 site, which is currently the topic of debate as to whether it is an additional high-affinity binding site for substrate molecules and whether its occupation with an additional substrate is important for the transport process.[20] Meanwhile, structures of LeuT with other substrates and inhibitors have been reported in addition to an open-to-out structure of LeuT.[21]

Only two investigations have so far analyzed the binding of small molecules in the S1 site of GAT1 using docking and subsequent molecular dynamics (MD)[22] or flexible docking,[23] and were able to predict the biological activities of a small set of analyzed compounds. In both studies the nitrogen atom of nipecotic acid was found to point to the intracellular gate of GAT1. A modeling study using MD calculations to compare the binding of nipecotic acid and tiagabine came to the same conclusion that nipecotic acid is bound to GAT1 in an orientation by which the amino nitrogen atom faces mainly the intracellular side of the GAT1 protein.[24] In contrast, the N-substituted nipecotic acid moiety in tiagabine is oriented with its nitrogen atom facing the extracellular side, and the lipophilic group is oriented into the vestibule (S2 site).

Table 1. pK_i and pIC_{50} values for GAT1 binding and inhibition and docking results.[a]

Entry	Compd	pK_i[29]	pIC_{50}[30]	AutoDock4 pK_i[b]
1	(*R*)-**5a**	4.50±0.05	5.19±0.03	4.43
2	(*R*)-**5b**	3.53±0.06	3.72±0.09	4.99
3	(*R*)-**5c**	6.33±0.04	5.49±0.09	6.68
4	(*R*)-**5d**	7.43±0.11	6.88±0.12	7.02
5	(*S*)-**5a**	2.99±0.05	4.24±0.05	4.34
6	(*S*)-**5b**	3.05±0.09	3.12±0.15	5.08
7	(*S*)-**5c**	5.64±0.11	4.97±0.10	6.86
8	(*S*)-**5d**	6.94±0.13	6.20±0.13	6.78
9	**6a**	3.75±0.09	4.87±0.06	4.53
10	**6b**	2.84±0.04	3.10±0.03	5.01
11	**6c**	6.32±0.23	5.22±0.16	6.99
12	**6d**	7.04±0.06	6.61±0.09	6.51
13	(*S*)-**7a**	4.25±0.02	5.57±0.03	4.65
14	(*S*)-**7b**	2.86±0.03	3.21±0.03	4.83
15	(*S*)-**7c**	6.61±0.13	5.99±0.11	5.88
16	(*S*)-**7d**	6.98±0.09	6.69±0.01	6.62
17	(*R*)-**8a**	0.27[c]	1.60±0.03	4.44
18	(*R*)-**8b**	2.50±0.13	2.32±0.15	4.59
19	(*R*)-**8c**	5.83±0.04	5.42±0.06	6.41
20	(*R*)-**8d**	6.44±0.07	6.43±0.11	6.37
21	(*S*)-**8a**	1.68±0.10	2.93±0.10	4.01
22	(*S*)-**8b**	1.66±0.01	1.69±0.09	4.55
23	(*S*)-**8c**	6.16±0.14	5.24±0.06	6.11
24	(*S*)-**8d**	6.79±0.03	6.01±0.10	6.07
25	(*R*)-**9a**	2.61±0.05	3.62±0.08	4.87
26	(*R*)-**9b**	2.47±0.02	2.73±0.21	4.78
27	(*R*)-**9c**	6.24±0.05	4.90±0.16	6.70
28	(*R*)-**9d**	6.65±0.06	6.04±0.07	6.07
29	(*S*)-**9a**	2.60±0.12	3.39±0.17	4.83
30	(*S*)-**9b**	3.60±0.03	3.52±0.09	4.72
31	(*S*)-**9c**	7.13±0.03	6.64±0.05	6.35
32	(*S*)-**9d**	6.75±0.03	6.24±0.03	6.47
33	(*R*)-**1**[d]	7.43±0.11	6.88±0.12	7.02

[a] All biological testing results were processed and evaluated in triplicate; Each pIC_{50} and pK_i value is the mean ±SEM of three independent experiments. [b] AutoDock4 pK_i was calculated from the AutoDock4 estimated inhibition constant K_i, which is reported in the AutoDock4 output. [c] Single experiment performed in triplicate; due to the high concentration required, the obtained value is of limited reliability. [d] Tiagabine.

The data regarding binding affinities and inhibitory potential toward GAT1 determined by uptake assays of pure amino acids and those N-substituted with 4,4-diphenylbut-3-en-1-yl (DPB) and 4,4-bis(3-methylthiophen-2-yl)but-3-en-1-yl (BTB) groups clearly indicate that the gain in binding energy brought by adding a large bulky lipophilic residue to small amino acids does not show a linear correlation. In contrast, the gain in inhibitory potential and binding affinity by adding the same group, for example, BTB, to small amino acids raises the measured values by one to nearly five log units. This large mis-

match is likely to indicate that some of the unsubstituted amino acids, like (*R*)-nipecotic acid [(*R*)-**5a**] or guvacine (**6a**), for which the gain in binding energy is relatively low, adopt a favorable binding pose, yielding high binding affinities. Such poses cannot be adopted if a bulky substituent is attached to the nitrogen atom, an assumption that is underscored by the few molecular modeling investigations available so far.

To clarify the hypothesis that small and large binders of GAT1 use partly different binding modes, we investigated a set of small cyclic amino acids {(*R*)-nipecotic acid [(*R*)-**5a**], (*S*)-nipecotic acid [(*S*)-**5a**], guvacine (**6a**), 2-[(3*S*)-pyrrolidin-3-yl]acetic acid [(*S*)-**7a**], (*R*)- and (*S*)-proline [(*R*)-**8a** and (*S*)-**8a**], and (*R*)- and (*S*)-2-(-pyrrolidin-2-yl)acetic acid [(*R*)-**9a** and (*S*)-**9a**]} and their DPB-, BTB-, and butyl-substituted derivatives (Figure 2).

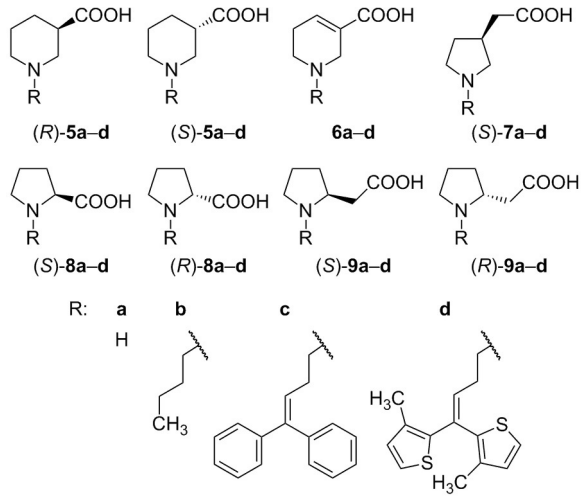

Figure 2. The selected amino acids and substituents.

The binding affinities of the pure amino acids range from $pK_i = 0.27$ for (*R*)-**8a** up to $pK_i = 4.50$ for (*R*)-**5a** for GAT1 binding (~ 4.2 log units; compare entry 17 with entry 1 in Table 1), whereas the pK_i values for the BTB-substituted compounds are all within one log unit of $pK_i = 6.44–7.43$ (for (*R*)-**8d** and (*R*)-**5d**; compare entry 20 with entry 4 in Table 1). Some preliminary docking calculations indicated that amino acids substituted at the nitrogen atom are able to occupy the main binding pocket (S1) of GAT1, but that in the presence of a substituent of a certain size, such as an *N*-butyl residue, the amino group points toward the extracellular side of GAT1, whereas the pure amino acids investigated by Palló et al.[22] and Wein et al.,[23] according to these authors, adopt orientations with the nitrogen atom pointing to the intracellular side of the protein. Therefore, we wanted to identify the binding and inhibition values of *N*-butyl-substituted compounds in order to delineate possible recommendations for the fragment-based drug design for new GAT1 inhibitors.

Results

Synthesis

To be able to compare the biological activity of the N-unsubstituted amino acids and their butyl derivatives with those of the large inhibitors at GAT1 in uptake and binding assays, first the respective compounds, i.e., butyl- [(*R*)-**5b**, (*S*)-**5b**, **6b**, (*S*)-**7b**, (*S*)-**8b**, (*R*)-**8b**, (*S*)-**9b**, (*R*)-**9b**], DPB- [**6c** and (*S*)-**7c**] and BTB-substituted compounds [(*S*)-**5d**, (*S*)-**7d** and (*R*)-**8d**] had to be synthesized. The synthesis of the new *N*-butyl derivatives was accomplished by reductive amination, except in the case of **6b**, for which a nucleophilic substitution strategy was applied, as the double bond already present in the guvacine moiety could suffer under the conditions of reductive amination. Thus, (*R*)-**5b**, (*S*)-**5b**, (*S*)-**8b**, and (*R*)-**8b** were synthesized directly from the respective commercially available amino acids (Scheme 1) by treatment with butyraldehyde applying hydrogen (5 bar) in the presence of pallidum on charcoal. Pyrrolidin-3-yl-acetic acid derived N-butylated compound (*S*)-**7b**, and pyrrolidin-2-yl-acetic acid derivatives (*S*)-**9b** and (*R*)-**9b** were also obtained by reductive amination, albeit by starting from the respective CBz-protected amino acids **10**,[25] (*S*)-**11**, and (*R*)-**11**, respectively, accomplishing deprotection and N-substitution with the butyric moiety in "one pot" (Scheme 1).

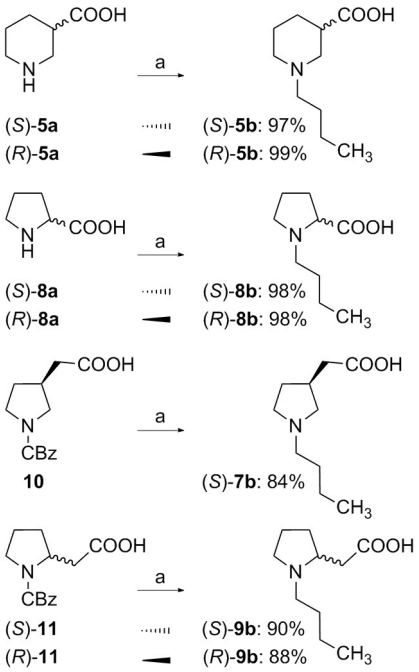

Scheme 1. Synthesis of *N*-butyl amino acids via reductive amination. *Reagents and conditions*: a) H_2 (5 bar), Pd/C, butyraldehyde, EtOH, RT.

The novel compounds bearing an olefinic moiety, either in the amino acid (**6b** and **6c**) or in the substituents to be attached [(*S*)-**5d**·HCl, (*S*)-**7c**, and (*S*)-**7d**], were synthesized by means of a conventional nucleophilic substitution reaction. Thus, treatment of (*S*)-ethyl piperidine-3-carboxylate (**12**) or

1,2,5,6-tetrahydropyridine-3-carboxylic acid methyl ester (**14**) with the respective alkyl bromide [1-bromobutane (**22b**) or 4,4-diphenylbut-3-en-1-yl bromide (**22c**)] in the presence of catalytic amounts of KI and K_2CO_3 as base gave the N-substituted amino acid methyl ester **13d** (70%) and **15b** (57%). The following alkaline hydrolysis of these ester functions in **13d** and **15b**, as well as in **15c**[16c] provided amino acids **6b**, **6c**, and (*S*)-**5d**·HCl (Scheme 2).

Compounds (*S*)-**7c** and (*S*)-**7d** were synthesized starting from Boc-protected amino acid **16**. At first **16** was transformed into the respective ester **17** by treatment with methyl iodide. Removal of the Boc group of **17** with TFA gave amino acid methyl ester hydrotrifluoromethanesulfonate **18**, which was subjected to nucleophilic substitution with either **22c** (4,4-diphenylbut-3-en-1-yl bromide) or **22d** [(4,4-bis(3-methylthiophen-2-yl)but-3-en-1-]yl bromide, to afford N-substituted amino acid esters **19c** and **19d**, respectively. Subsequent hydrolysis with 12 M NaOH yielded the desired amino acids (*S*)-**7c** and (*S*)-**7d**. Finally, (*R*)-**8d** was synthesized similarly by starting from (*R*)-proline methyl ester hydrochloride (**20**), introducing the [(4,4-bis(3-methylthiophen-2-yl)but-3-en-1-]yl moiety by treating **20** with bromide **22d** to give **21d** which, after hydrolysis, yielded the desired proline derivative (*R*)-**8d** (85%, Scheme 2).

All other compounds required for this study that carry either a 4,4-diphenylbut-3-en-1-yl [(*S*)-**5c**, (*R*)-**5c**,[16c] (*S*)-**8c**, (*R*)-**8c** (*S*)-**9c**, (*R*)-**9c**],[17] or [(4,4-bis(3-methylthiophen-2-yl)but-3-en-1-]yl substituent [(*R*)-**5d**,[16c] **6d**,[26] (*S*)-**8d**, (*S*)-**9d**, (*R*)-**9d**[17] were reported previously, and have been synthesized following published procedures.

Biological data

In the following, the binding affinities (pK_i values) are discussed in detail, but the conclusions drawn are equally well supported by the observed pIC_{50} values from the uptake assays, which are listed in Table 1 as well, for the sake of completeness. The N-unsubstituted amino acids (*R*)- and (*S*)-**5a**, **6a**, (*S*)-**7a**, (*R*)- and (*S*)-**8a**, and (*R*)- and (*S*)-**9a** show pK_i values between 0.27 and 4.50 (Table 1, entries 1, 5, 9, 13, 17, 21, 25, 29). When linked with a DPB residue, the resulting compounds (*R*)-**5c**, (*S*)-**5c**, **6c**, (*S*)-**7c**, (*R*)-**8c**, (*S*)-**8c**, (*R*)-**9c**, and (*S*)-**9c** show remarkably high binding affinities to GAT1, with pK_i values in the range of 5.64–7.13 (Table 1, entries 3, 7, 11, 15, 19, 23, 27, 31), no matter whether the corresponding unsubstituted amino acids possess low or high binding affinities. Even more remarkable are the BTB-substituted compounds (*R*)-**5d**, (*S*)-**5d**, **6d**, (*S*)-**7d**, (*R*)-**8d**, (*S*)-**8d**, (*R*)-**9d**, and (*S*)-**9d**, which exhibit binding affinities with pK_i values between 6.44 and 7.43 (Table 1, entries 4, 8, 12, 16, 20, 24, 28, 32). The only exception where the DPB derivative shows a slightly higher pK_i than the BTB substituted compound (*S*)-**9b** is (*S*)-**9c** (Table 1, compare entry 31 and entry 32). These experimental results indicate that the pure amino acids with low binding affinities (pK_i) and low inhibition values (pIC_{50}) gain much more binding potential from the DPB or BTB substituents than amino acids with already high binding affinities or inhibition values.

The GAT1 binding values of the *N*-butyl derivatives [(*R*)- and (*S*)-**5b**, **6b**, (*S*)-**7b**, (*R*)- and (*S*)-**8b**, (*R*)-**9b**, and (*S*)-**9b**] are all in a range between 1.66 and 3.60 (Table 1, entries 2, 6, 10, 14, 18, 22, 26, 30). The binding constants of N-unsubstituted amino

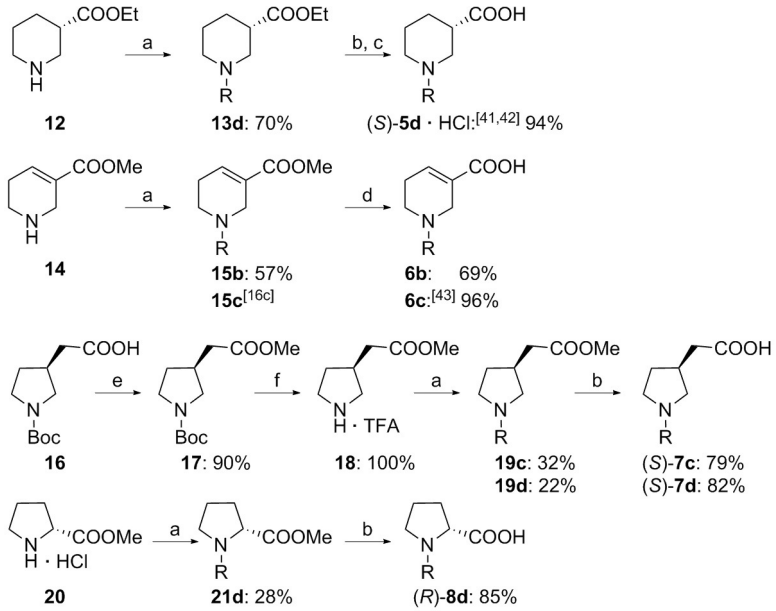

Scheme 2. Synthesis of N-substituted amino acids via nucleophilic substitution. *Reagents and conditions*: a) 1-bromobutane (**22b**), 4,4-diphenylbut-3-en-1-yl bromide (**22c**) or [(4,4-bis(3-methylthiophen-2-yl)but-3-en-1-]yl bromide (**22d**), KI, K_2CO_3, acetone, RT; b) aq. NaOH/EtOH; c) HCl (2 M); d) $Ba(OH)_2 \cdot 8H_2O$, EtOH/H_2O 1:1 (*v*/*v*); e) CH_3I, K_2CO_3, DMF, RT; f) TFA, CH_2Cl_2, RT. The synthesis of compounds (*S*)-**5d**·HCl[26] and its free base[27] as well as **6c**[28] were reported previously, but no spectroscopic data were made available.

acids, which are already good binders like (*R*)-nipecotic acid [(*R*)-**5a**, pK_i = 4.50, entry 1], guvacine (**6a**, pK_i = 3.75, entry 9), and 2-[(3*S*)-pyrrolidin-3-yl]acetic acid [(*S*)-**7a**, pK_i = 4.25, entry 13], are decreased by 0.97, 0.91, and 1.59 log units, respectively, indicating that these amino acids might be forced to adopt a new binding mode by the butyl group. On the other hand, the low pK_i value (0.27) of (*R*)-proline (*R*)-**8a** (Table 1, entry 17) is dramatically increased by adding the butyl group. The butyl-substituted proline (*R*)-**8b** exhibits a pK_i value of 2.50 (Table 1, entry 18), which is now in the same range as the pK_i values for the other butyl-substituted compounds.

Notably, the small good binders (*R*)-**5a**, **6a**, and (*S*)-**7a**, (entries 1, 9, 13) lose binding affinity when N-substituted, whereas the binding values of the small moderate and weak binders (*S*)-**5a**, (*S*)-**8a**, (*R*)-**9a**, and (*S*)-**9a**, (entries 5, 21, 25, 29) do not change very much. These findings seem to indicate that (*R*)-nipecotic acid [(*R*)-**5a**], guvacine (**6a**), and (*S*)-pyrrolidin-3-yl-acetic acid [(*S*)-**7a**] bind GAT1 in a very favorable binding pose which cannot be adopted if they are N-substituted with a butyl or bulkier substituent such as DPB or BTB. In contrast, the binding affinities of the small moderate or weak binders are not significantly affected by N-substitution with the butyl substituent except for (*R*)-**8a**, for which this results in a gain and not a loss of binding affinity. When N-substituted with a BTB or DPB residue, all of the parent amino acids show a gain in binding affinity, the increase of which is, however, often strikingly different.

Docking

To get a more detailed view of potential binding modes that explain the measured pK_i values, we conducted a series of docking calculations using homology models of GAT1 as the target. The first available 3D protein structure of a homologous transporter protein was the leucine transporter from *Aquifex aeolicus* (LeuT$_{Aa}$, PDB ID: 2A65).[19] The structure includes a substrate leucine molecule trapped in an active site almost in the middle of the protein, called the S1 site. The protein conformation in 2A65 is called "closed" because the active site S1 is not accessible from the extracellular or intracellular sides. Some years after the aforementioned structure had been reported, a LeuT structure with a so-called "open-to-out" conformation was published (PDB ID: 3F3A)[21c] in which the S1 site was open and accessible from the extracellular side. This open S1 site, the S2 site, and the channel to the extracellular water was occupied with two tryptophan molecules, one detergent molecule, and three water molecules. We calculated homology models of GAT1 based on either the "closed" conformation (PDB ID: 2A65) or the "open-to-out" conformation of LeuT (PDB ID: 3F3A). Subsequent docking calculations revealed that the binding energies from the docking calculations obtained using the "open-to-out" GAT1 model did not correspond as well with the experimental pK_i values as the docking binding energies using the "closed" GAT1 model. However, as all BTB- or DPB-substituted amino acids [(*R*)-**5c**, (*S*)-**5c**, **6c**, (*S*)-**7c**, (*S*)-**8c**, (*R*)-**8c**, (*S*)-**9c**, (*R*)-**9c**, (*R*)-**5d**, (*S*)-**5d**, **6d**, (*S*)-**7d**, (*S*)-**8d**, (*R*)-**8d**, (*S*)-**9d**, and (*R*)-**9d**] did not fit into the "closed" S1 site of GAT1 without significant overlap with protein atoms and large energy penalties, we investigated the binding while keeping the gate-keeping side chains of the residues Phe293, Tyr140, Arg69, and Asp451 flexible in order to obtain meaningful results. The binding energies calculated with AutoDock4 were converted into pK_i values and are listed in Table 1.

For all unsubstituted amino acids [(*R*)-**5a**, (*S*)-**5a**, **6a**, (*S*)-**7a**, (*S*)-**8a**, (*R*)-**8a**, (*S*)-**9a**, and (*R*)-**9a**,] that fit into the S1 site, the best-scoring poses represent an orientation in which the nitrogen atom in the ring is directed toward the intracellular side of the protein, which is in accordance with previous results of Palló et al.,[22] Wein et al.,[23] and Skovstrup et al.[24] The carboxylic acid moiety of all parent amino acids interacts with the sodium atom Na1. The nitrogen atom of (*R*)- and (*S*)-nipecotic acid [(*R*)-**5a** and (*S*)-**5a**], guvacine (**6a**) and 2-[(3*S*)-pyrrolidin-3-yl]acetic acid [(*S*)-**7a**] is part of two hydrogen bonds to Tyr60-C=O and Tyr60-OH oxygen. (*R*)- and (*S*)-proline [(*R*)-**8a** and (*S*)-**8a**], (2*S*)-pyrrolidin-2-yl-acetic acid and 2-(2*R*)-pyrrolidin-2-yl-acetic acid [(*S*)-**9a** and (*R*)-**9a**] are unable to adopt a conformation in which their nitrogen atom is part of two hydrogen bonds to Tyr60. In their case, their amino group can only interact with the backbone oxygen atom of Phe293-C=O, a fact that explains the lower pIC_{50} and pK_i values observed in the biological tests (Figure 3).

For docking runs with butyl-substituted compounds [(*R*)-**5b**, (*S*)-**5b**, **6b**, (*S*)-**7b**, (*R*)-**8b**, (*S*)-**8b**, (*R*)-**9b**, and (*S*)-**9b**] the two gate-keeping residues Tyr140 and Phe294 were kept flexible during docking. All of these derivatives adopt orientations with the butyl group, and hence the nitrogen atom of the amino acids, pointing toward the extracellular side, which is exemplarily shown in Figure 4 for *N*-butyl derivative (*R*)-**5b** in compari-

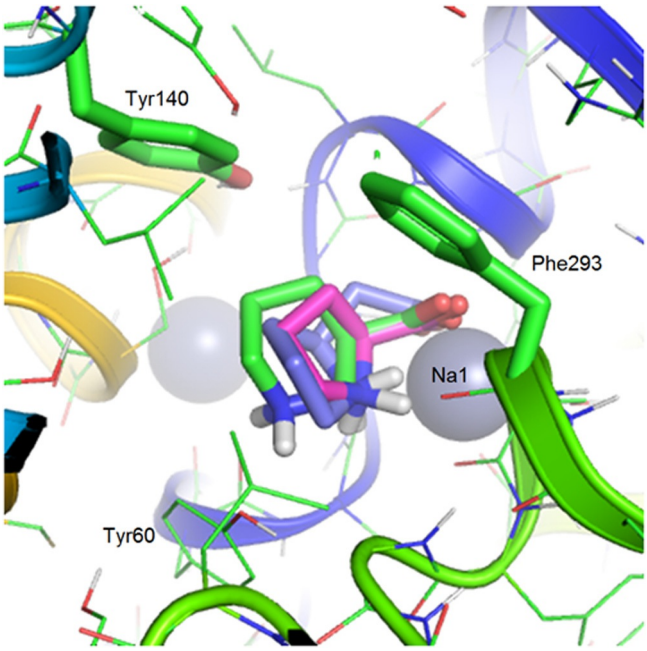

Figure 3. Best docking poses in the "closed" S1 site: (*R*)-nipecotic acid (*R*)-**5a** in green, (*S*)-proline (*S*)-**8a** in magenta, 2-[(2*S*)-pyrrolidin-2-yl]acetic acid (*S*)-**9a** in blue.

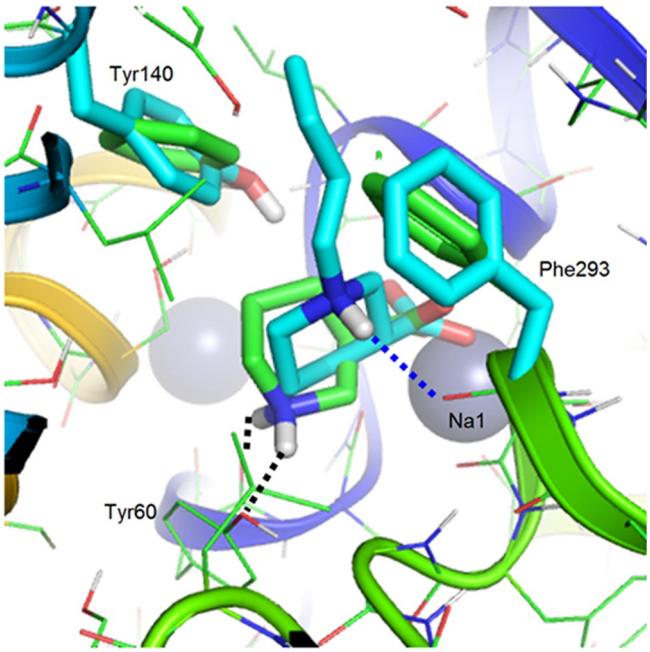

Figure 4. Results from docking into the "closed" GAT1 conformation with the side chains of Tyr140 and Phe293 flexible (shown as stick models): (*R*)-nipecotic acid (*R*)-**5a** in green and (*R*)-*N*-butylnipecotic acid (*R*)-**5b** in cyan. The important hydrogen bonds between nipecotic acid and Tyr60-C=O and Tyr60-OH are depicted with dotted black lines. The hydrogen bond between *N*-butylnipecotic acid and Phe293-C=O is shown with a dotted blue line.

son with the N-unsubstituted compound (*R*)-**5a**. In the case of (*R*)-**5b**, only one hydrogen bond between the NH hydrogen and Phe294-C=O is possible in this orientation, whereas for (*R*)-**5a** it had been two (to Tyr60).

The compounds with BTB or DPB substituents still do not fit into this model or only with a high energy penalty, rendering the results unreasonable. For the BTB- and DPB-substituted compounds it is necessary to open the channel even more by making Tyr140 and Phe293 and the salt bridge Arg69 and Asp451 flexible during docking in order to get negative scoring energies. With this setup, docking experiments are able to differentiate between the weak binders like the pure amino acids [(*R*)-**5a**, (*S*)-**5a**, **6a**, (*S*)-**7a**, (*R*)-**8a**, (*S*)-**8a**, (*R*)-**9a**, and (*S*)-**9a**] and *N*-butyl-substituted compounds [(*R*)-**5b**, (*S*)-**5b**, **6b**, (*S*)-**7b**, (*R*)-**8b**, (*S*)-**8b**, (*R*)-**9b**, and (*S*)-**9b**] on one side, and the good binders like the DPB- [(*R*)-**5c**, (*S*)-**5c**, **6c**, (*S*)-**7c**, (*R*)-**8c**, (*S*)-**8c**, (*R*)-**9c**, (*S*)-**9c**] and BTB-substituted compounds [(*R*)-**5d**, (*S*)-**5d**, **6d**, (*S*)-**7d**, (*R*)-**8d**, (*S*)-**8d**, (*R*)-**9d**, (*S*)-**9d**] on the other. In addition, it nicely reproduces the rank order of binding potency for the BTB-substituted compounds [(*R*)-**5d**, (*S*)-**5d**, **6d**, (*S*)-**7d**, (*R*)-**8d**, (*S*)-**8d**, (*R*)-**9d**, (*S*)-**9d**]. Again, as with the *N*-butyl-substituted compounds, for the DPB- and BTB-substituted compounds the only hydrogen bond for the NH hydrogen that exists is toward Phe293-C=O.

Discussion

(*R*)-Nipecotic acid [(*R*)-**5a**], guvacine (**6a**), and 2-[(3*S*)-pyrrolidin-3-yl]acetic acid [(*S*)-**7a**] are known to be good inhibitors and binders of GAT1. Their N-substituted derivatives with 4,4-diphenylbut-3-en-1-yl (DPB) [(*R*)-**5c**, **6c**, (*S*)-**7c**] or with 4,4-bis(3-methylthiophen-2-yl)but-3-en-1-yl (BTB) [(*R*)-**5d**, **6d**, (*S*)-**7d**] residues show some of the highest inhibition of GAT1 known so far. However, the gain in affinity due to the addition of the N-substituents, the DPB or the BTB residue, is only in the range of 1.84–2.56 (for DPB) and 2.73–3.29 (for BTB) log units. In stark contrast, the very poor inhibitors of GAT1, such as (*R*)- and (*S*)-proline [(*R*)-**8a** and (*S*)-**8a**] or (*R*)- and (*S*)-2-(-pyrrolidin-2-yl)acetic acid[17] [(*R*)-**9a** and (*S*)-**9a**] gain between 3.64 to 5.55 (DPB) and 4.05 to 6.17 (BTB) log units if N-substituted with DPB [(*R*)-**8c** and (*S*)-**8c**, (*R*)-**9c** and (*S*)-**9c**] or BTB [(*R*)-**8d** and (*S*)-**8d**, (*R*)-**9d** and (*S*)-**9d**] groups. This marked difference in gain in binding affinity, a low increase for the more potent and a high increase for the less potent N-unsubstituted amino acids, suggest that either the binding mode of the N-unsubstituted good binders or even of both the good and weak binders, do not reflect the orientation these amino acids adopt when substituted with DPB and BTB residues. In other words, at least the N-unsubstituted amino acids that exhibit high binding affinities display a binding pose that provides a high binding affinity, but is not related to the orientation of this unit in the DPB- and BTB-substituted derivatives. Consequently, the high binding affinities that these N-unsubstituted amino acids possess cannot be transmitted into the DPB- and BTB-substituted derivatives.

The high inhibitory power of the known small GAT1 inhibitors, i.e., of (*R*)-nipecotic acid [(*R*)-**5a**], guvacine (**6a**), and 2-[(3*S*)-pyrrolidin-3-yl] acetic acid [(*S*)-**7a**] seems to be based on the fact that these compounds might be able to accommodate a perfect fit into the closed site S1 in GAT1 where the nitrogen atom is directed toward the intracellular side of the channel forming hydrogen bonds with the carbonyl and side chain oxygen atoms of Tyr60 (Figure 4). The synthesis of the *N*-butyl-substituted derivatives of the investigated amino acids was performed, as it was expected that as soon as a substituent like an *N*-butyl group is present, the nitrogen atom of the amino acids must be oriented toward the extracellular side of the protein. This way all small amino acid inhibitors of mGAT1 should be forced into a binding pose with an orientation similar to that of the amino acid and linker part of the large amino acid GAT1 inhibitors, the latter of which differ largely from the former only by the additional presence of the aromatic residues. As a consequence thereof, the binding affinities shown by the *N*-butyl-substituted amino acids should more reliably reflect their potential to serve as starting points for the development of large mGAT1 inhibitors with aromatic residues. Indeed, this appears to be the case. The variance of the gain in binding energy for the transition from the *N*-butyl- to *N*-diarylbutenyl-substituted amino acids acting as GAT1 binders is far smaller, ranging from 2.59 to 4.50 log units for the DPB and from 3.15 to 5.13 log units for the BTB residue than before for the N-unsubstituted versus the DPB- (1.84–5.55 log units) and BTB-substituted compounds (2.73–6.17 log units). This is also plausible taking the results from the docking experiments into account. The strong small amino acid binders (*R*)-nipecotic acid [(*R*)-**5a**], guvacine (**6a**), and 2-[(3*S*)-pyrrolidin-3-yl]acetic

acid [(*S*)-**7a**] profit from favorable interactions with Tyr60 comprising two hydrogen bonds. Upon substitution of the amino nitrogen with alkyl residues such as an *N*-butyl moiety or larger groups and the resulting reorientation of the system, this favorable interaction is lost, and only one hydrogen bond can be formed. Although the docking model used is able to predict almost the order of potency of the BTB-substituted compounds and can distinguish the small versus large binders, the subtle differences between the pure amino acids and the *N*-butyl compounds is not reproduced. However, the above-mentioned effect is clearly observed in the pK_i values of the N-butylated amino acids (*R*)-**5b**, **6b**, and (*S*)-**7b** (Table 1, entries 2, 10, 14) which decrease between one and more than two orders of magnitude. In contrast, unsubstituted amino acids that have no or only low inhibitory potency toward GAT1 such as (*R*)-**5a**, (*S*)-**5a**, (*S*)-**8a**, (*R*)-**9a**, and (*S*)-**9a** (Table 1, entries 1, 5, 17, 21, 25, 29), the inhibition (pK_i) values are not changed very much upon *N*-butyl substitution [(*S*)-**5b**, (*S*)-**8b**, (*R*)-**9b**; entries 6, 18, 26] or are even increased [(*R*)-**5b**, (*S*)-**9b**], as in their case the orientation of the amino group toward the intracellular side associated with the interaction with Tyr60 is not strongly favored or is not favored at all.

Conclusions

Docking studies have underlined the hypothesis that the nitrogen atom of N-unsubstituted nipecotic acid [(*R*)-**5a** and (*S*)-**5a**] is oriented toward the intracellular side of the binding pocket, and, in contrast, the substituted nitrogen atom of *N*-butylnipecotic acid or tiagabine must be oriented toward the extracellular side. In consequence, a fragment-based approach for the construction of potent GAT1 inhibitors must take possible different binding modes of the amino acid fragments into consideration, depending on the substitution of the amino nitrogen. Small N-unsubstituted amino acids with already high binding potential may not gain as much binding potential as those with very low values, whereas small amino acids with low or very low binding activity can be transformed into very good binders. Considering the fact that N-butyl-substituted amino acids, although only displaying a small N-substituent, always adopt a binding pose with the amino nitrogen pointing toward the extracellular side, which is thus analogous to that of the large binders, this investigation suggests that fragments already carrying an N-butyl substituent represent a much more valid basis for the design of new potent inhibitors.

Experimental Section

Homology modeling

For homology modeling of a "closed" GAT1 conformation, the 3D structure of PDB ID: 2A65[19] was taken from the RCSB Protein Data Bank.[31] The only available 3D structure of an "open-to-out" conformation (PDB ID: 3F3A[21c]) was chosen as a template for an "open" GAT1 conformation. The human GAT1 sequence (SwissProt[32] accession number P30531) was aligned to the LeuT sequence using the alignment from Skovstrup et al.[24] Modeller software version 9v8[33] was used to generate 30 structures of each conformer. The two sodium atoms (Na1 and Na2) located close to the S1 binding site were copied into the hGAT1 structures. A chloride ion was placed into the putative chloride binding site proposed by Zomot et al.[34] and Forrest et al.[35] However, the chloride ion has no direct contact to the active site, and its presence has no impact on the docking calculations. The models with the lowest Modeller objective function were checked with PROCHECK[36] for structural consistency and further used for docking calculations.

Docking

The molecules for docking were exported from our in-house Instant JChem 5.4 database[37] as 2D MDL .mol files. Protonation at pH 7.4 and the 2D-to-3D conversion was done using ChemAxon Marvin 5.4.0.1[38] "cxcalc" and "molconvert". The command line tool "prepare_dpf42.py" was used for conversion into AutoDock4 .pdbqt input files. Appropriate protein input files were prepared with AutoDock tools.[39] Docking grids were calculated with "autogrid4", and docking was performed with AutoDock4 version 4.2.3.[40] The binding region was defined by a $18\times18\times18$ Å^3 box centered between the two gate-keeping residues Tyr140 and Phe294. Ten poses for each molecule were generated and scored with the AutoDock4 scoring function.[40b]

Synthesis

Anhydrous reactions were carried out in vacuum-dried glassware under a nitrogen or argon atmosphere. CH_3CN was freshly distilled from CaH_2 and EtOH from sodium under nitrogen with addition of diethyl phthalate. Other common solvents were p.a. quality or freshly distilled before use. The phosphate buffer (pH 7) was prepared by dissolving $NaH_2PO_4{\cdot}H_2O$ (77.32 g) and $Na_2HPO_4{\cdot}2\,H_2O$ (58.36 g) in H_2O (1 L).

Purchased reagents were used without further purification. TLC was carried out using plates purchased from Merck (silica gel 60 F_{254} on aluminum sheet). Column chromatography (CC) was carried out using Merck silica gel 60 (mesh 0.040–0.063 mm) as stationary phase. Compounds were stained with 5% $(NH_4)_6Mo_7O_{24}{\cdot}4\,H_2O$, 0.2% $Ce(SO_4)_2{\cdot}4\,H_2O$, and 5% concd H_2SO_4. Optical rotation: Polarimeter 241 MC, Polarimeter ADP440+ at $\lambda=589$ cm^{-1}. Melting points: mp (uncorrected) were determined with a Büchi 510 Melting Point apparatus. IR spectroscopy: FT-IR Spectrometer 1600 and Paragon 1000 (PerkinElmer), oils were measured as film, solid samples as KBr pellets for measurements. Mass spectrometry: Mass spectrometer 5989 A with 59980 B particle beam LC–MS interface (Hewlett Packard). High-resolution (HR) mass spectrometry was performed on either a Thermo Finnigan LTQ FT (ESI) or a JMS GCmate II JEOL (EI). ^{1}H and ^{13}C NMR spectra were recorded with a JNMR-GX (JEOL, 400 or 500 MHz) using TMS or dioxane as internal standard and integrated with the MestReNova (Version 5.2.5-4119, Mestrelab Research S.L., 2008).

Synthesis and experimental data of compounds (*S*)-**5d**·HCl, **6c**, (*S*)-**7c**, (*S*)-**7d**, (*R*)-**8d**, **13d**, **19c**, **19d**, and **21d** are provided in the Supporting Information.

General Procedure 1 (GP1): A mixture of the respective amino acid (1 equiv) and butyraldehyde (1.2 mmol) in absolute EtOH (10 mL) under argon atmosphere was hydrogenated at 5 bar in the presence of 10% Pd/C (50 mg) for the time given. The suspension was filtered, washed with EtOH, and the filtrate was evaporated under reduced pressure.

General Procedure 2 (GP2): The respective ester derivative (1 equiv) in EtOH (0.5 M) was cooled to 0 °C, and aqueous NaOH (12 M, 2 equiv) was added dropwise. The ice bath was removed, and the resulting mixture was stirred at room temperature for the time given. The reaction mixture was again cooled to 0 °C and acidified (pH ≈ 6) using HCl (0.25 M). H_2O was then added, followed by extraction with CH_2Cl_2. The combined organic layers were dried over $MgSO_4$ and concentrated in vacuo.

(*R*)-1-Butylpiperidine-3-carboxylic acid [(*R*)-5 b]: Prepared according to GP1 starting from (*R*)-(−)-nipecotic acid (129 mg, 1.0 mmol) and butyraldehyde (86.5 mg, 1.2 mmol); reaction time: 4 h. Yield: 184 mg (99%) white solid; mp: 84–86 °C; $[\alpha]_D^{20}$ +10.5° (*c* = 0.21 in MeOH); ^{1}H NMR (500 MHz, NaOD in D_2O): δ = 0.89 (t, *J* = 7.4 Hz, 3H, CH_3), 1.23–1.32 (m, 1H, NCH_2CHCH_2), 1.23–1.32 (m, 2H, CH_3CH_2), 1.43–1.54 (m, 2H, $CH_3CH_2CH_2$), 1.43–1.54 (m, 1H, $NCH_2CHCH_2CH_2$), 1.68–1.73 (m, 1H, $NCH_2CHCH_2CH_2$), 1.87–1.96 (m, 1H, NCH_2CHCH_2), 1.87–1.96 (m, 1H, NCH_2CH), 1.87–1.96 (m, 1H, $CH(CH_2)_2CH_2$), 2.30–2.36 (m, 1H, NCH_2CH), 2.30–2.36 (m, 2H, $CH_3(CH_2)_2CH_2$), 2.89 (d_{br}, *J* = 11.9 Hz, 1H, $CH(CH_2)_2CH_2$), 3.02–3.05 ppm (m, 1H, NCH_2CH); ^{13}C NMR (125 MHz, NaOD in D_2O): δ = 13.9 (CH_3), 21.0 (CH_3CH_2), 24.7 ($CH(CH_2)_2CH_2$), 28.3 ($CH_3CH_2CH_2$), 28.5 (NCH_2CHCH_2), 45.5 (NCH_2CH), 53.5 ($CH(CH_2)_2CH_2$), 56.5 (NCH_2CH), 58.7 ($CH_3(CH_2)_2CH_2$), 184.1 ppm (*C*=O); IR (film): $\tilde{\nu}$ = 3396, 2957, 2874, 1698, 1588, 1453, 1410, 1359, 1120 cm^{-1}; MS (CI, CH_5^+) *m/z* (%): 186 (100) $[M+H]^+$, 168 (6), 142 (8); HRMS-EI+ *m/z* $[M]^+$ calcd for $C_{10}H_{19}N_1O_2$: 185.1416, found: 185.1418.

(*S*)-1-Butylpiperidine-3-carboxylic acid [(*S*)-5 b]: Prepared according to GP1 starting from (*S*)-(+)-nipecotic acid (129 mg, 1.0 mmol) and butyraldehyde (86.5 mg, 1.2 mmol); reaction time 4 h. Yield: 180 mg (97%) white solid; mp: 85–87 °C. Analytical data (^{1}H NMR, ^{13}C NMR, IR, MS) are in accordance with those of the *R* enantiomer (*R*)-**5 b**; $[\alpha]_D^{20}$ −11.4° (*c* = 0.21 in MeOH).

Methyl 1-butyl-1,2,5,6-tetrahydropyridine-3-carboxylate (15 b): 1,2,5,6-Tetrahydropyridine-3-carboxylic acid methyl ester (**14**)[41] (212 mg, 1.5 mmol) was stirred with K_2CO_3 (829 mg, 6.0 mmol), KI (50 mg, 0.3 mmol) and 1-bromobutane (**22 b**, 411 mg, 3.0 mmol) in dry acetone (6 mL) at room temperature for 24 h. The solvent was evaporated, then water was added, and the solution was extracted with CH_2Cl_2 (3×6 mL). The organic layers were collected, dried over Na_2SO_4 and concentrated. The residue was purified by flash chromatography over silica gel (*n*-heptane/Et_2O 7:3, 1% *N*-ethyldimethylamine, R_f = 0.2). Yield: 169 mg (57%) yellow oil: ^{1}H NMR (400 MHz, $CDCl_3$): δ = 0.93 (t, *J* = 7.3 Hz, 3H, CH_3), 1.30–1.39 (m, 2H, CH_3CH_2), 1.51–1.58 (m, 2H, $CH_3CH_2CH_2$), 2.33–2.38 (m, 2H, $CHCH_2$), 2.45–2.49 (m, 2H, $CH_3(CH_2)_2CH_2$), 2.53 (t, *J* = 5.7 Hz, 2H, $CHCH_2CH_2$), 3.18–3.19 (m, 2H, NCH_2C), 6.99–7.02 ppm (m, 1H, CHC); ^{13}C NMR (100 MHz, $CDCl_3$): δ = 14.1 (CH_3), 20.8 (CH_3CH_2), 26.6 ($CHCH_2$), 29.2 ($CH_3CH_2CH_2$), 49.1 (NCH_2CC), 51.5 ($CHCH_2CH_2$), 51.6 (OCH_3), 58.2 ($CH_3(CH_2)_2CH_2$), 129.0 (*C*CH), 138.0 (C*C*H), 166.4 ppm (*C*=O); IR (film): $\tilde{\nu}$ = 2954, 2932, 2872, 2807, 2765, 1717, 1657, 1437, 1262, 1194, 1141, 1089, 1048, 719 cm^{-1}; MS (CI, CH_5^+) *m/z* (%): 198 (100) $[M+H]^+$, 168 (2), 154 (10), 141 (2); HRMS-EI+ *m/z* $[M]^+$ calcd for $C_{11}H_{19}N_1O_2$: 197.1416, found: 197.1407.

1-Butyl-1,2,5,6-tetrahydropyridine-3-carboxylic acid (6 b): Methyl 1-butyl-1,2,5,6-tetrahydropyridine-3-carboxylate (**15 b**, 70 mg, 0.35 mmol) was stirred with $Ba(OH)_2{\cdot}8H_2O$ (221 mg, 0.70 mmol) in EtOH/H_2O (1:1; 2.8 mL) at room temperature overnight. Dry ice was then added until precipitation of barium was complete, and the resulting milky suspension was filtered and concentrated. Yield: 44 mg (69%) white solid; mp: 105–108 °C; ^{1}H NMR (500 MHz, $CDCl_3$): δ = 0.94 (t, *J* = 7.4 Hz, 3H, CH_3), 1.33–1.40 (m, 2H, CH_3CH_2), 1.73–1.79 (m, 2H, $CH_3CH_2CH_2$), 2.47–2.53 (m, 2H, $CHCH_2$), 2.93–2.97 (m, 2H, $CH_3(CH_2)_2CH_2$), 3.07–3.13 (m, 2H, $CHCH_2CH_2$), 3.72–3.77 (m, 2H, NCH_2C), 6.84–6.86 ppm (m, 1H, CHC); ^{13}C NMR (125 MHz, $CDCl_3$): δ = 13.7 (CH_3), 20.3 (CH_3CH_2), 22.5 ($CHCH_2$), 26.1 ($CH_3CH_2CH_2$), 47.3 ($CHCH_2CH_2$), 49.8 (NCH_2CC), 55.2 ($CH_3(CH_2)_2CH_2$), 129.6 (*C*CH), 131.0 (C*C*H), 170.0 ppm (*C*=O); IR (KBr): $\tilde{\nu}$ = 3440, 2961, 2935, 2875, 1671, 1583, 1364, 734 cm^{-1}; MS (CI, CH_5^+) *m/z* (%): 184 (100) $[M+H]^+$, 166 (7), 140 (9), 86 (2); HRMS-EI+ *m/z* $[M]^+$ calcd for $C_{10}H_{17}N_1O_2$: 183.1259, found: 183.1221.

(*S*)-2-(1-Butylpyrrolidin-3-yl)acetic acid [(*S*)-7 b]: Prepared according to GP1 starting from (*S*)-2-{1-[(benzyloxy)carbonyl]pyrrolidin-3-yl}acetic acid (**10**, 144 mg, 0.55 mmol) and butyraldehyde (59.8 mg, 0.83 mmol) in absolute EtOH (4.3 mL); reaction time: 24 h. Yield: 85 mg (84%) light-yellow solid; mp: 51–53 °C; $[\alpha]_D^{20}$ −7.3° (*c* = 0.45 in MeOH); ^{1}H NMR (500 MHz, CD_3OD): δ = 0.99 (t, *J* = 7.4 Hz, 3H, CH_3CH_2), 1.39–1.47 (m, 2H, CH_3CH_2), 1.66–1.72 (m, 2H, $CH_3CH_2CH_2$), 1.77 (dq, *J* = 13.3, 8.7 Hz, 1H, NCH_2CHCH_2), 2.25–2.31 (m, 1H, NCH_2CHCH_2), 2.33 (dd, *J* = 15.7, 7.1 Hz, 1H, $CHCH_2CO$), 2.42 (dd, *J* = 15.7, 5.7 Hz, 1H, $CHCH_2CO$), 2.66–2.75 (m, 1H, NCH_2CH), 3.09–3.18 (m, 2H, $N(CH_2)_2CH_2$), 3.09–3.18 (m, 1H, NCH_2CH), 3.21–3.27 (m, 1H, $CHCH_2CH_2$), 3.40–3.48 (m, 1H, $CHCH_2CH_2$), 3.40–3.48 ppm (m, 1H, NCH_2CH); ^{13}C NMR (125 MHz, CD_3OD): δ = 14.0 (CH_3CH_2), 21.0 (CH_3CH_2), 29.2 ($CH_3CH_2CH_2$), 30.2 (NCH_2CHCH_2), 35.3 (NCH_2CH), 42.3 ($CHCH_2CO$), 54.9 ($CHCH_2CH_2$), 55.7 ($N(CH_2)_2CH_2$), 60.1 (NCH_2CH), 179.5 ppm (*C*O); IR (film): $\tilde{\nu}$ = 3428, 2964, 2935, 2875, 1745, 1702, 1627, 1418, 1386, 1288, 1245 cm^{-1}; MS (CI, CH_5^+) *m/z* (%): 186 (46) $[M+H]^+$, 129 (66), 111 (100); HRMS-ESI+ *m/z* $[M+H]^+$ calcd for $C_{10}H_{20}N_1O_2$: 186.1494, found: 186.1489.

(*S*)-1-Butylpyrrolidine-2-carboxylic acid [(*S*)-8 b]: Prepared according to GP1 starting from L-proline [(*S*)-**8 a**, 115 mg, 1.0 mmol] and butyraldehyde (86.5 mg, 1.2 mmol); reaction time: 5 h. Yield: 168 mg (98%) light-yellow solid; mp: 71–73 °C; $[\alpha]_D^{20}$ −56.6° (*c* = 0.47 in MeOH); ^{1}H NMR (400 MHz, CD_3OD): δ = 0.98 (t, *J* = 7.4 Hz, 3H, CH_3), 1.42 (sextet, *J* = 7.3 Hz, 2H, CH_3CH_2), 1.62–1.77 (m, 2H, $CH_3CH_2CH_2$), 1.88–2.00 (m, 1H, $CHCH_2CH_2$), 2.04–2.16 (m, 1H, $CHCH_2CH_2$), 2.04–2.16 (m, 1H, $CHCH_2$), 2.37–2.47 (m, 1H, $CHCH_2$), 3.05–3.13 (m, 1H, $CH(CH_2)_2CH_2$), 3.05–3.13 (m, 1H, $CH_3(CH_2)_2CH_2$), 3.20–3.27 (m, 1H, $CH_3(CH_2)_2CH_2$), 3.73 (ddd, *J* = 11.2, 7.3, 3.7 Hz, 1H, $CH(CH_2)_2CH_2$), 3.84 ppm (dd, *J* = 9.3, 6.0 Hz, 1H, NCH); ^{13}C NMR (100 MHz, CD_3OD): δ = 14.0 (CH_3), 21.0 (CH_3CH_2), 24.5 ($CHCH_2CH_2$), 29.0 ($CH_3CH_2CH_2$), 30.4 ($CHCH_2$), 56.1 ($CH(CH_2)_2CH_2$), 56.6 ($CH_3(CH_2)_2CH_2$), 70.8 (NCH), 173.6 ppm (C=O); IR (film): $\tilde{\nu}$ = 3406, 2962, 2937, 2875, 1624, 1459, 1389 cm^{-1}; MS (CI, CH_5^+) *m/z* (%): 172 (100) $[M+H]^+$, 126 (15); HRMS-EI+ *m/z* $[M]^+$ calcd for $C_9H_{17}N_1O_2$: 171.1259, found: 171.1256.

(*R*)-1-Butylpyrrolidine-2-carboxylic acid [(*R*)-8 b]: Prepared according to GP1 starting from D-proline [(*R*)-**8 a**, 115 mg, 1.0 mmol] and butyraldehyde (86.5 mg, 1.2 mmol); reaction time: 5 h. Yield: 168 mg (98%) light-yellow solid; mp: 71–73 °C; Analytical data (^{1}H NMR, ^{13}C NMR, IR, MS) are in accordance with those of the *S* enantiomer (*S*)-**8 b**; $[\alpha]_D^{20}$ +58.1° (*c* = 0.47 in MeOH).

(*S*)-2-(1-Butylpyrrolidin-2-yl)acetic acid [(*S*)-9 b]: Prepared according to GP1 starting from (*S*)-2-{1-[(benzyloxy)carbonyl]pyrrolidin-2-yl}acetic acid[42] [(*S*)-**11**, 105 mg, 0.4 mmol] and butyraldehyde (43.3 mg, 0.6 mmol) in absolute EtOH (3 mL); reaction time: 24 h. Yield: 66 mg (90%) light-yellow solid; mp: 76–77 °C; $[\alpha]_D^{20}$ −101.3°; (*c* = 0.15 in MeOH); ^{1}H NMR (400 MHz, CD_3OD): δ = 1.00 (t, *J* = 7.4 Hz, 3H, CH_3), 1.35–1.52 (m, 2H, CH_3CH_2), 1.65–1.76 (m, 2H, $CH_3CH_2CH_2$), 1.78–1.87 (m, 1H, $CHCH_2CH_2$), 1.98–2.14 (m, 2H, $CHCH_2CH_2$), 2.25–2.34 (m, 1H, $CHCH_2CH_2$), 2.50 (dd, *J* = 16.6, 3.8 Hz, 1H, CH_2CO), 2.70 (dd, *J* = 16.6, 5.6 Hz, 1H, CH_2CO), 2.93–2.99 (m,

1H, $CH_3(CH_2)_2CH_2$), 3.11 (dt, J=11.4, 8.0 Hz, 1H, $CH(CH)_2CH_2$), 3.33–3.39 (m, 1H, $CH_3(CH_2)_2CH_2$), 3.53–3.59 (m, 1H, NC*H*), 3.65–3.72 ppm (m, 1H, $CH(CH)_2CH_2$); ^{13}C NMR (125 MHz, CD_3OD): δ=14.0 (CH_3), 21.0 (CH_3CH_2), 23.2 ($CHCH_2CH_2$), 29.2 ($CH_3CH_2CH_2$), 30.5 ($CHCH_2CH_2$), 35.8 (CH_2CO), 54.0 ($CH(CH_2)_2CH_2$), 54.1 ($CH_3(CH_2)_2CH_2$), 66.7 (NCH), 177.7 ppm (C=O); IR (KBr): $\tilde{\nu}$=3434, 2963, 2937, 2876, 1593, 1468, 1448, 1379, 1366, 1036, 704 cm^{-1}; MS (CI, CH_5^+) *m/z* (%): 186 (100) $[M+H]^+$, 142 (4), 126 (63); HRMS-EI+ *m/z* $[M]^+$ calcd for $C_{10}H_{19}N_1O_2$: 185.1416, found: 185.1407.

(*R*)-2-(1-Butylpyrrolidin-2-yl)acetic acid [(*R*)-9 b]: Prepared according to GP1 starting from (*R*)-2-{1-[(benzyloxy)carbonyl]pyrrolidin-2-yl}acetic acid[1] ([(*R*)-**11**, 118 mg, 0.45 mmol) and butyraldehyde (48.7 mg, 0.67 mmol) in absolute EtOH (3.5 mL); reaction time: 24 h. Yield: 73 mg (88%) light-yellow solid; mp: 76–77 °C; Analytical data (^{1}H NMR, ^{13}C NMR, IR, MS) are in accordance with those of the *S* enantiomer (*S*)-**9 b**. $[\alpha]_D^{20}$ +101.7° (*c*=0.27 in MeOH); HRMS-EI+ *m/z* $[M]^+$ calcd for $C_{10}H_{19}N_1O_2$: 185.1416, found: 185.1427.

(*S*)-*tert*-Butyl 3-(2-methoxy-2-oxoethyl)pyrrolidine-1-carboxylate (17): (*S*)-2-(1-(*tert*-Butoxycarbonyl)pyrrolidin-3-yl)acetic acid (**16**, 230 mg, 1.00 mmol) dissolved in DMF (3.0 mL) was stirred with K_2CO_3 (416 mg, 3.0 mmol) and CH_3I (456 mg 3.2 mmol) at room temperature for 66 h. The solvent volume was significantly decreased in vacuo, and H_2O (10 mL) was added. The aqueous phase was extracted with EtOAc (5×10 mL), and the combined organic layers were washed once with H_2O (10 mL), $Na_2S_2O_3$ solution (10%, 10 mL) and brine (10 mL) then dried (Na_2SO_4), filtered and concentrated in vacuo. Yield: 219 mg (90%) orange oil: $[\alpha]_D^{20}$ +25.3° (*c*=0.7 in MeOH); ^{1}H NMR (400 MHz, $CDCl_3$, 50 °C): δ=1.46 (s, 9H, $(CH_3)_3$), 1.56 (m, 1H, NCH_2CH_2), 2.05 (m, 1H, NCH_2CH_2), 2.30–2.47 (m, 2H, NCH_2CH, CH_2COO), 2.56 (m, 1H, CH_2COO), 2.95 (m, 1H, NCH_2CH) 3.30 (m, 1H, NCH_2CH_2), 3.44 (m, 1H, NCH_2CH_2), 3.59 (m, 1H, NCH_2CH), 3.68 ppm (s, 3H, OCH_3); ^{13}C NMR (100 MHz, $CDCl_3$, 50 °C): δ=28.6 ($(CH_3)_3$), 31.0 (NCH_2CH_2), 35.0 (CH_2COO), 37.6 (NCH_2CH), 45.2 (NCH_2CH_2), 51.2 (NCH_2CH), 51.6 (OCH_3), 79.2 ($C(CH_3)_3$), 154.6 (NC=O), 172.5 ppm (CO); IR (KBr): $\tilde{\nu}$=3447, 2960, 2780, 2495, 1736, 1678, 1439, 1202 cm^{-1}; MS (ESI+) *m/z*: 244 $[M+H]^+$; HRMS-ESI+ *m/z* $[M+H]^+$ calcd for $C_{12}H_{22}NO_4$: 244.1543, found: 336.1953.

(*S*)-3-(2-Methoxy-2-oxoethyl)pyrrolidin-1-ium trifluoroacetate (18): To (*S*)-*tert*-butyl 3-(2-methoxy-2-oxoethyl)pyrrolidine-1-carboxylate (**17**, 204 mg, 0.838 mmol) dissolved in CH_2Cl_2 (4.8 mL) was added TFA (744 mg, 6.53 mmol) at 0 °C. The ice bath was removed, and the mixture was stirred for 17 h at room temperature. The solvent and excess TFA were removed in vacuo. Yield: 216 mg (100%) yellow oil: $[\alpha]_D^{20}$ +11.8° (*c*=0.5 in MeOH); ^{1}H NMR (400 MHz, CD_3OD, 19 °C): δ=1.67 (dq, J=12.8, 9.0 Hz, 1H, NCH_2CH_2), 2.25 (dtd, J=12.8, 7.3, 4.2 Hz, 1H, NCH_2CH_2), 2.53 (dd, J=16.7, 8.0 Hz, 1H, CH_2COO), 2.60 (dd, J=16.7, 6.4 Hz, 1H, CH_2COO), 2.67 (m, 1H, CH_2CH), 2.91 (dd, J=11.8, 8.9 Hz, 1H, NCH_2CH_2), 3.23 (ddd, J=11.6, 9.2, 7.6 Hz, 1H, NCH_2CH), 3.38 (ddd, J=11.6, 8.5, 4.2 Hz, 1H, NCH_2CH), 3.53 (dd, J=11.8, 7.6 Hz, 1H, NCH_2CH_2), 3.68 ppm (s, 3H, OCH_3); ^{13}C NMR (100 MHz, $CDCl_3$, 50 °C): δ=31.0 (NCH_2CH_2), 35.5 (NCH_2CH), 37.1 (CH_2CO), 46.2 (NCH_2CH_2), 50.9 (NCH_2CH), 52.3 (OCH_3), 173.7 ppm (CO); IR (KBr): $\tilde{\nu}$=2976, 2875, 1739, 1695, 1407, 1166 cm^{-1}; MS (ESI+) *m/z*: 144 $[M+H]^+$, 401 $[2M+TFA+H]^+$; HRMS-ESI+ *m/z* $[M+H]^+$ calcd for $C_7H_{14}NO_2$: 144.1019, found: 144.1019.

Keywords: docking · GABA transporter · GAT1 · homology modeling · tiagabine

[1] M. Palacín, R. Estévez, J. Bertran, A. Zorzano, *Physiol. Rev.* **1998**, *78*, 969–1054.

[2] a) Y. Zhou, S. Holmseth, R. Hua, A. C. Lehre, A. M. Olofsson, I. Poblete-Naredo, S. A. Kempson, N. C. Danbolt, *Am. J. Physiol.: Renal. Physiol.* **2012**, *302*, F316–F328; b) Y. Zhou, S. Holmseth, C. Guo, B. Hassel, G. Hofner, H. S. Huitfeldt, K. T. Wanner, N. C. Danbolt, *J. Biol. Chem.* **2012**, *287*, 35733–35746.

[3] a) Q. R. Liu, B. López-Corcuera, S. Mandiyan, H. Nelson, N. Nelson, *J. Biol. Chem.* **1993**, *268*, 2106–2112; b) Y. Zhou, N. C. Danbolt, *Front. Endocrinol.* **2013**, *4*, 165.

[4] K. K. Madsen, H. S. White, A. Schousboe, *Pharmacol. Ther.* **2010**, *125*, 394–401.

[5] a) J. Masson, C. Sagné, M. Hamon, S. E. Mestikawy, *Pharmacol. Rev.* **1999**, *51*, 439–464; b) F. Chen, M. B. Larsen, H. A. Neubauer, C. Sánchez, P. Plenge, O. Wiborg, *J. Neurochem.* **2005**, *92*, 21–28; c) U. Gether, P. H. Andersen, O. M. Larsson, A. Schousboe, *Trends Pharmacol. Sci.* **2006**, *27*, 375–383; d) A. S. Kristensen, J. Andersen, T. N. Jorgensen, L. Sorensen, J. Eriksen, C. J. Loland, K. Stromgaard, U. Gether, *Pharmacol. Rev.* **2011**, *63*, 585–640; e) T. Kvist, B. Christiansen, A. A. Jensen, H. Bräuner-Osborne, *Comb. Chem. High Throughput Screening* **2009**, *12*, 241–249.

[6] P. Krogsgaard-Larsen, E. Falch, O. M. Larsson, A. Schousboe, *Epilepsy Res.* **1987**, *1*, 77–93.

[7] H. Nelson, S. Mandiyan, N. Nelson, *FEBS Lett.* **1990**, *269*, 181–184.

[8] J. Guastella, N. Nelson, H. Nelson, L. Czyzyk, S. Keynan, M. C. Miedel, N. Davidson, H. A. Lester, B. I. Kanner, *Science* **1990**, *249*, 1303–1306.

[9] a) B. S. Meldrum, A. G. Chapman, *Epilepsia* **1999**, *40*, S2–6; b) N. O. Dalby, *Eur. J. Pharmacol.* **2003**, *479*, 127–137.

[10] P. D. Suzdak, K. Frederiksen, K. E. Andersen, P. O. Sorensen, L. J. Knutsen, E. B. Nielsen, *Eur. J. Pharmacol.* **1992**, *224*, 189–198.

[11] L. M. Yunger, P. J. Fowler, P. Zarevics, P. E. Setler, *J. Pharmacol. Exp. Ther.* **1984**, *228*, 109–115.

[12] M. R. Pavia, S. J. Lobbestael, D. Nugiel, D. R. Mayhugh, V. E. Gregor, C. P. Taylor, R. D. Schwarz, L. Brahce, M. G. Vartanian, *J. Med. Chem.* **1992**, *35*, 4238–4248.

[13] C. K. Thoeringer, S. Ripke, P. G. Unschuld, S. Lucae, M. Ising, T. Bettecken, M. Uhr, M. E. Keck, B. Mueller-Myhsok, F. Holsboer, E. B. Binder, A. Erhardt, *J. Neural Transm.* **2009**, *116*, 649–657.

[14] G. X. Liu, G. Q. Cai, Y. Q. Cai, Z. J. Sheng, J. Jiang, Z. Mei, Z. G. Wang, L. Guo, J. Fei, *Neuropsychopharmacology* **2007**, *32*, 1531–1539.

[15] a) P. Krogsgaard-Larsen, *Mol. Cell. Biochem.* **1980**, *31*, 105–121; b) P. Krogsgaard-Larsen, G. A. R. Johnston, *J. Neurochem.* **1975**, *25*, 797–802; c) G. A. Johnston, P. Krogsgaard-Larsen, A. L. Stephanson, B. Twitchin, *J. Neurochem.* **1976**, *26*, 1029–1032.

[16] a) L. Nielsen, L. Brehm, P. P. Y. Krogsgaard-Larsen, *J. Med. Chem.* **1990**, *33*, 71–77; b) O. M. Larsson, P. Thorbek, P. Krogsgaard-Larsen, A. Schousboe, *J. Neurochem.* **1981**, *37*, 1509–1516; c) F. E. Ali, W. E. Bondinell, P. A. Dandridge, J. S. Frazee, E. Garvey, G. R. Girard, C. Kaiser, T. W. Ku, J. J. Lafferty, G. I. Moonsammy, H.-J. Oh, J. A. Rush, P. E. Setler, O. D. Stringer, J. W. Venslavsky, B. W. Volpe, L. M. Yunger, C. L. Zirkle, *J. Med. Chem.* **1985**, *28*, 653–660.

[17] G. H. Fülep, C. E. Hoesl, G. Höfner, K. T. Wanner, *Eur. J. Med. Chem.* **2006**, *41*, 809–824.

[18] a) M. Sindelar, T. A. Lutz, M. Petrera, K. T. Wanner, *J. Med. Chem.* **2013**, *56*, 1323–1340; b) G. Quandt, G. Hofner, K. T. Wanner, *Bioorg. Med. Chem.* **2013**, *21*, 3363–3378.

[19] A. Yamashita, S. K. Singh, T. Kawate, Y. Jin, E. Gouaux, *Nature* **2005**, *437*, 215–223.

[20] a) C. L. Piscitelli, H. Krishnamurthy, E. Gouaux, *Nature* **2010**, *468*, 1129–1132; b) S. K. Singh, A. Yamashita, E. Gouaux, *Nature* **2007**, *448*, 952–956; c) T. Beuming, J. Kniazeff, M. L. Bergmann, L. Shi, L. Gracia, K. Raniszewska, A. H. Newman, J. A. Javitch, H. Weinstein, U. Gether, C. J. Loland, *Nat. Neurosci.* **2008**, *11*, 780–789; d) M. Quick, L. Shi, B. Zehnpfennig, H. Weinstein, J. A. Javitch, *Nat. Struct. Mol. Biol.* **2012**, *19*, 207–211; e) M. Quick, A.-M. L. Winther, L. Shi, P. Nissen, H. Weinstein, J. A. Javitch, *Proc. Natl. Acad. Sci. USA* **2009**, *106*, 5563–5568; f) L. Shi, M. Quick, Y. Zhao, H. Weinstein, J. A. Javitch, *Mol. Cell* **2008**, *30*, 667–677.

[21] a) E. Gouaux, *Philos. Trans. R. Soc. London Ser. B* **2009**, *364*, 149–154; b) H. Krishnamurthy, E. Gouaux, *Nature* **2012**, *481*, 469–474; c) S. K. Singh, C. L. Piscitelli, A. Yamashita, E. Gouaux, *Science* **2008**, *322*, 1655–1661.

[22] A. Palló, A. Bencsura, L. Héja, T. Beke, A. Perczel, J. Kardos, A. Simon, *Biochem. Biophys. Res. Commun.* **2007**, *364*, 952 – 958.
[23] T. Wein, K. T. Wanner, *J. Mol. Model.* **2010**, *16*, 155 – 161.
[24] S. Skovstrup, O. Taboureau, H. Bräuner-Osborne, F. S. Jørgensen, *ChemMedChem* **2010**, *5*, 986 – 1000.
[25] J. Eustache, A. Grob, C. Lam, O. Sellier, G. Schulz, *Bioorg. Med. Chem. Lett.* **1998**, *8*, 2961 – 2966.
[26] K. E. Andersen, C. Braestrup, F. C. Gronwald, A. S. Jorgensen, E. B. Nielsen, U. Sonnewald, P. O. Sorensen, P. D. Suzdak, L. J. Knutsen, *J. Med. Chem.* **1993**, *36*, 1716 – 1725.
[27] "N-Substituted Azaheterocyclic Carboxylic Acids and Their Esters", W. E. Bondinell, J. J. Lafferty, C. L. Zirkle (Smithkline Beckman Corp.), Eur. Pat. No. EP 0066456 A1, **1982**.
[28] "Preparation of Tiagabine, Its (*S*)-Isomer, and Racemate", J. Zhang, C. Jiang, R. Wen, G. Lin (Shanghai Institute of Organic Chemistry, Chinese Academy of Sciences), Pat. No. CN1651426A, **2005**.
[29] a) C. Zepperitz, G. Höfner, K. T. Wanner, *ChemMedChem* **2006**, *1*, 208 – 217; b) G. Höfner, K. T. Wanner, *J. Chromatogr. B* **2010**, *878*, 1356 – 1364.
[30] A. Kragler, G. Höfner, K. T. Wanner, *Eur. J. Med. Chem.* **2008**, *43*, 2404 – 2411.
[31] H. M. Berman, J. Westbrook, Z. Feng, G. Gilliland, T. N. Bhat, H. Weissig, I. N. Shindyalov, P. E. Bourne, *Nucleic Acids Res.* **2000**, *28*, 235 – 242.
[32] B. Boeckmann, A. Bairoch, R. Apweiler, M.-C. Blatter, A. Estreicher, E. Gasteiger, M. J. Martin, K. Michoud, C. O'Donovan, I. Phan, S. Pilbout, M. Schneider, *Nucleic Acids Res.* **2003**, *31*, 365 – 370.
[33] M.-Y. Shen, A. Sali, *Protein Sci.* **2006**, *15*, 2507 – 2524.
[34] E. Zomot, A. Bendahan, M. Quick, Y. Zhao, J. A. Javitch, B. I. Kanner, *Nature* **2007**, *449*, 726 – 730.
[35] L. R. Forrest, S. Tavoulari, Y.-W. Zhang, G. Rudnick, B. Honig, *Proc. Natl. Acad. Sci. USA* **2007**, *104*, 12761 – 12766.
[36] R. A. Laskowski, M. W. Macarthur, D. S. Moss, J. M. Thornton, *J. Appl. Crystallogr.* **1993**, *26*, 283 – 291.
[37] Instant JChem, version 5.4, ChemAxon, **2010**: https://www.chemaxon.com/products/instant-jchem-suite/instant-jchem/.
[38] Marvin, version 5.4.0.1, ChemAxon, **2010**: https://www.chemaxon.com/products/marvin/.
[39] M. F. Sanner, *J. Mol. Graphics Modell.* **1999**, *17*, 57 – 61.
[40] a) G. M. Morris, D. S. Goodsell, R. S. Halliday, R. Huey, W. E. Hart, R. K. Belew, A. J. Olson, *J. Comput. Chem.* **1998**, *19*, 1639 – 1662; b) R. Huey, G. M. Morris, A. J. Olson, D. S. Goodsell, *J. Comput. Chem.* **2007**, *28*, 1145 – 1152.
[41] I. Coldham, K. M. Crapnell, J. C. Fernandez, J. D. Moseley, R. Rabot, *J. Org. Chem.* **2002**, *67*, 6181 – 6187.
[42] J. M. Cassal, A. Furst, W. Meier, *Helv. Chim. Acta* **1976**, *59*, 1917 – 1924.

Received: November 13, 2015
Published online on January 25, 2016